PRZEGLĄD ELEKTROTECHNICZNY

OPEN ACCESS

Daoud SEKKI[1], Hakim AZIZI[2], Mohammed CHEBOUT[3], Mohammed Charif KIHAL[4], Marouane KIHAL[5]

ORCID: [1]0009-0003-2204-7459, [3]0009-0003-4895-6327, [3]0009-0006-2798-5411, [4]0000-0002-2075-2491, [5]0000-0002-6675-708

DOI: 10.15199/48.2025.08.09

Modeling and measurement of the propagation of carrier currents in lines on MV/LV transformers equipped with its power lines

Modelowanie i pomiar propagacji prądów nośnych w domowej sieci elektrycznej zawierającej linie energetyczne i transformator napięcia średniego/podstawowego (MV/LV)

[1] Daoud SEKKI, Laboratory of Research on Electromechanical and Dependability, Souk Ahras University, Souk Ahras, Algeria, e-mail: daoud.sekki@univ-soukahras

[2] Hakim AZIZI, Energy Systems Applications Laboratory, Ziane Achour University, Djelfa, Algeria, e-mail: h.azizi@univ-djelfa.dz

[3] Mohammed CHEBOUT, Applied Automation and industrial Diagnostic Laboratory, Ziane Achour University, Djelfa, Algeria, e-mail: m.chebout@univ-djelfa.dz

[4] Mohammed Charif KIHAL, L2EI Laboratory, Mohamed Seddik Ben Yahia University, Jijel, Algeria, e-mail: mc.kihal@univ-jijel.dz

[5] Marouane KIHAL is with the Mohamed Boudiaf, M'sila, Algeria, e-mail: marouane.kihal@univ-bejaia.dz

Correspondence address: daoud.sekki@univ-soukahras

Abstract: In this paper, we study the propagation of the on-line carrier currents (PLC) on the domestic electrical network containing the power lines and the medium/base voltage transformer (MV/LV). To achieve this, we propose an efficient and precise modeling through the power transformer. Electrical energy is a physical quantity that can be measured in an unambiguously way, which is not the case for voltage and current. The bond graph analysis (integrated under SIMULINK (Matlab), based on energy and its conservation, appears to be the most suitable method for modeling low-level signal transmission. To demonstrate this advantage, we treat an application on a power transformer. The results obtained through numerical simulation are compared and validated by the measurement. Good agreements are found between this approach and measurement.

Keywords: Line carrier currents (PLC), Transformer (MV/LV), Measurement, EMTP-ATP software.

Streszczenie: W tym artykule badano propagację prądów nośnych on-line (PLC) w domowej sieci elektrycznej zawierającej linie energetyczne i transformator napięcia średniego/podstawowego (MV/LV). Aby to osiągnąć, proponuje się wydajne i precyzyjne modelowanie za pomocą transformatora mocy. Energia elektryczna jest wielkością fizyczną, którą można zmierzyć w sposób jednoznaczny, co nie jest prawdą w przypadku napięcia i prądu. Analiza wykresu wiązań (zintegrowana w ramach SIMULINK (Matlab), oparta na energii i jej zachowaniu, wydaje się być najbardziej odpowiednią metodą modelowania transmisji sygnału niskiego poziomu. Aby zademonstrować tę zaletę, autorzy rozpatrują aplikację w transformatorze mocy. Wyniki uzyskane za pomocą symulacji numerycznej są porównywane i weryfikowane za pomocą pomiaru. Znaleziono dobrą zgodność między tym podejściem a pomiarem.

Słowa kluczowe: Prądy nośne linii (PLC), transformator (SN/nn), pomiary, oprogramowanie EMTP-ATP.

Introduction

The transport of electrical energy from production centers to consumption centers is ensured by a complex network that connects all production centers and enables exchanges with foreign countries. This network allows for the continuous adjustment of production to match consumption, the technical and economic optimization of the production fleet, and the assurance of a reliable energy supply. This process, which is essential for electricity suppliers, is known as the operation of a production-transport system [1].

Unfortunately, the distribution network, which primarily consists of MV/LV transformers, is not designed to transmit high-frequency (HF) signals and may lead

to unforeseen situations for engineers. To prevent such issues, modeling the propagation of line carrier currents (PLC) in this network is an essential step. It helps engineers analyze signal attenuation, identify weak points in the network, and determine acceptable frequency bands for information transmission [2–5].

The purpose of PLC technology is to transmit data over electrical cables, which serve as carriers for data transmission. Unlike other communication media, such as Ethernet, coaxial cables, and optical fibers, the primary function of electrical cables is not data transmission [6]. Therefore, data transmission must coexist with the delivery of electrical energy, as these cables supply electrical equipment from the public power grid. Designed for widespread applications, PLC products must remain cost-effective, and modifications to the electrical grid connecting them should be minimized [7–9].

The electrical wiring used for power transmission was never designed to carry high-frequency (HF) signals. Experimental network results and the challenges in establishing corresponding standards confirm the presence of significant and critical losses and leaks. Modern wired telecommunications networks, on the other hand, use shielded cables, optical fibers, or symmetrical pairs, aiming to minimize signal leakage in interconnections and junction boxes [10].

Note also the presence of power transformers, which present in HF non-linearities to which are added a pronounced effect of eddy currents in the iron core, capacitive effects as well as resonance phenomena [11], [12].

In this work, we address the aforementioned problem by emphasizing the concepts of transfer function and, in particular, the power transmitted by high-frequency (HF) signals. Our objective is to analyze the propagation of PLC signals on power transmission lines and cables, as well as within the distribution network. The first goal relates to the need for a dedicated telecommunication system for the energy transmission network, requiring additional information to expand its scope and enhance its performance. The second goal concerns the injection of HF signals into the distribution network through the MV/LV transformer, which has become a reality, offering greater convenience (Internet, home automation, cable television, etc.), provided that certain obstacles are overcome [13,14].

Real Transformer

Figure 1 represents the equivalent electrical diagram of a transformer:

Where:

R_1: Primary winding wire resistance.

R_2: Secondary winding wire resistance.

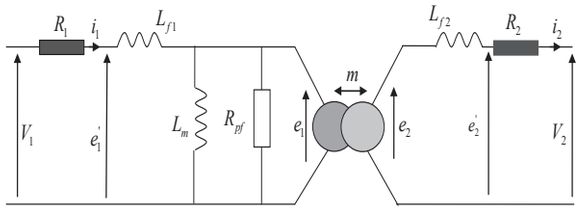

Fig. 1. Electrical diagram of a real single-phase transformer

m: Transformation ratio.

R_{pf}: Iron loss image resistance.

L_{mf}: Magnetizing inductance.

L_{f1} and L_{f2} are the primary and secondary leakage inductances, respectively.

High frequency transformer modeling

At (HF), even if the nonlinear effects of the iron core are neglected, transformer modeling becomes significantly more complex compared to its behavior at 50 Hz due to several phenomena:

- Effects of eddy currents in the iron core and in the coil conductors.
- Non-linear effect of iron core.
- Actions of the abilities that appear between coils and between coils and mass.
- Possibilities of resonance phenomena.

Detailed model

This type of model consists of representing the transformer by a large network of capacitances and inductances (figure 2). The calculation of its parameters requires the resolution of complex electromagnetic equations and information on the materials and detailed geometry of each transformer. As each turn is modeled in detail, this type of model is rather intended for the study of the voltage distribution in the windings [5]

Extensive research has been conducted to develop a universal model for high-frequency (HF) transformers. However, this goal remains far from being achieved due to the dependencies mentioned above,

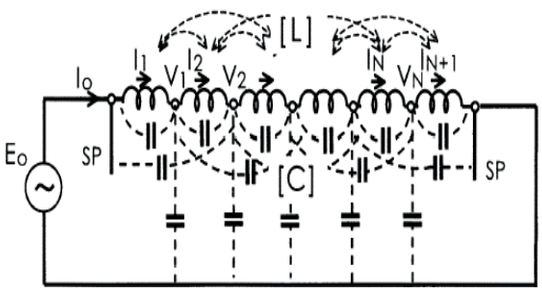

Fig. 2. Detailed equivalent circuit of a winding.

which stem from the varying structures of different transformers.

In practice, power transformer modeling is typically based either on transient analysis or on voltage distribution within the windings to design insulators that withstand over voltages. Consequently, transformer models can be categorized into two main approaches [5]:

CHIMKLAI model

In this work, the author builds upon a classical 50 Hz model, which consists of an ideal transformer, the winding resistance and inductance, and the magnetizing impedance. The extension to a high-frequency (HF) model is achieved by:

- Considering the frequency dependence of the winding's resistance and inductance, referred to as the winding impedance (as shown in figure 3). This impedance is synthesized using a nonlinear approximation method to derive an R, L, C circuit (Figure 2).
- Adding a system of capacitances, including the capacitance between the windings and the ground, the capacitance between the turns of a single winding, and the capacitance between the outer layers of different windings. All these capacitances are assumed to remain constant within the studied frequency range.

This work provides us with a good basis for developing our models of the HF transformer. However, there are still limitations: it assumes the phases are symmetrical, and the frequency up to which the model remains valid is 100 kHz.

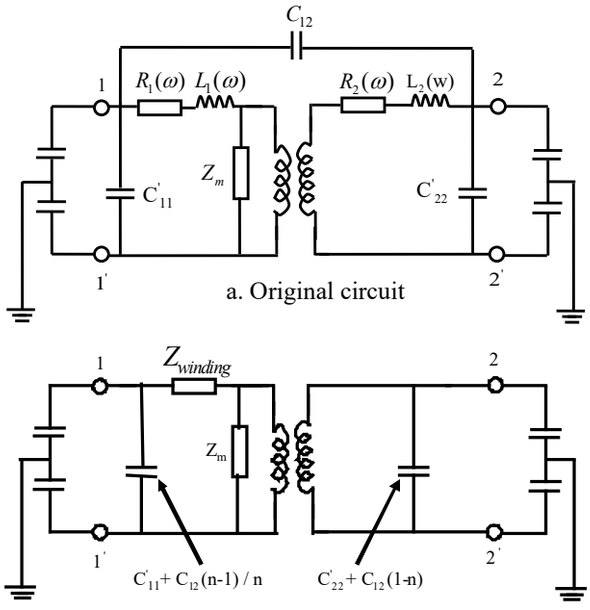

n: transformation ratio
b. simplified circuit

Fig. 3. S. Chimklai transformer model.

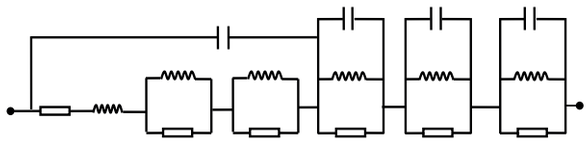

Fig. 4. Coil impedance

ANDRIEU model

In the work of C. Andrieu et al [2]. The proposed high frequency transformer model is considered as a black box with eight (08) connections as shown in figure 5:

- The primary side is a triangle with three (03) connections.
- The secondary side is star-shaped with four (04) connections and the last one is mass.

According to C. Andrieu the capacities in the high frequency transformer are divided into two types (figure 5):

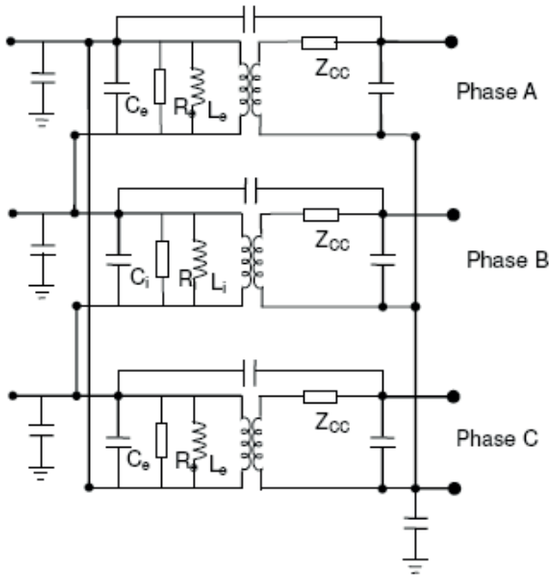

Fig. 5. Andrieu transformer model.

- Capabilities between the two primary and secondary conductors.
- Capabilities in the windings.

This model follows the same principles as that of S. Chimklai and takes into account:

- The capacities between the different windings.
- High voltage resonances.
- The low voltage winding impedance and its variation with frequency (Z_{cc}).

With:

Z_{cc}: Given by the following equivalent circuit (figure 4):

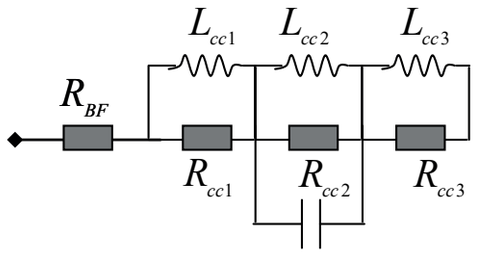

Fig. 6. Zcc equivalent circuit

Several measurements of the impedance of a power transformer as a function of frequency, published in the literature, have shown that from a certain frequency level, the iron core no longer plays a role in the measurement of impedance [3]

A. T. TRAN model

For frequencies above 100 kHz, the author suggests disregarding the iron core. A.T. Tran [3] therefore proposes eliminating the ideal transformer from the model originally proposed by S. Chimklai [1].

In this high-frequency (HF) transformer model (figure 7), only electrostatic phenomena and resonances are considered. To represent these phenomena, the model proposed by A.T. Tran [3] consists of:

- The capacities between the coils, and between the coils and the mass;
- The resonances of LV windings

With:

Z_f: Leakage impedance which represents the loss of flux that closes off outside the iron core.

C_1: Capacity between the outside of the coil and the ground. Several studies have shown that the latter can be divided into two capacities, each at one terminal of the coil.

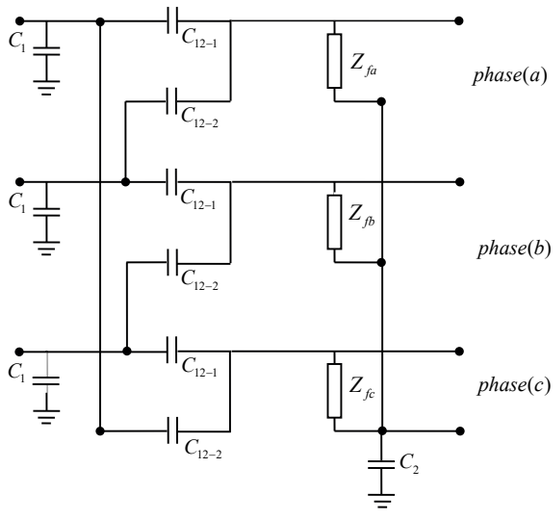

Fig. 7. A. T. Tran transformer model.

C_{12}: The capacitance between the inner and outer parts of the winding, represented by two parallel, non-identical capacitances.

The sharing rate of each capacity is determined by measurement and simulation work. But in principle, this rate reflects the arrangement of the windings and their geometric structure.

C_2: Capacity between the inside of the coil *BV* and the ground, this capacity comes from the fact that the iron core of the transformer is connected to the ground.

The parameters of this model are determined by different measurements; of resonances on the side which LV (Z_f) is represented by R-L-C a parallel circuit.

Determination of parameters

Leakage impedance Z_f

The frequency-dependent characteristic of the leakage impedance is obtained by measuring a short circuit. In fact, to represent this characteristic, we can use a parallel R, L circuit.

The impedance of a parallel R, L circuit is calculated by the formula as in equation:

$$Z = \frac{R}{1 - j\frac{R}{wL}} \tag{1}$$

When the frequency is very low |Z (f)| is practically linear, because $Z_L = w_L$ becomes small compared to R, Z » ZL = wL. So L can be calculated by the equation:

$$L = \frac{\Delta|Z(f)|}{2\pi.\Delta f} \tag{2}$$

The impedance of a parallel R, L, C circuit is calculated by the formula as in equation:

$$R = |Z(w_0)| \tag{3}$$

$$L = \frac{R}{Qw_0} \tag{4}$$

$$C = \frac{Q}{Rw_0} \tag{5}$$

With:

w0: resonant point angle velocity.

Q: quality factor, calculated in equation:

$$Q = \frac{f_0}{|f_{01} - f_{02}|} \tag{6}$$

With
f_0: frequency at the resonant point.
f_{01}, f_{02}: frequency at the -3dB point.

Electrical characteristics of the transformer

Figure 8 illustrates the geometry and structure of the transformer studied in this work. It is a three-phase transformer with two windings. The iron core has 3 columns and 2 sockets. For each phase, the primary (MV) and secondary (LV) are mounted on the same column, the MV is outside and the LV is inside.

Fig. 8.Transformer structure Model

To better understand the structure of the transformer, some details on the tests are shown in table 1.

Table. 1 Transformer test parameters

Nominal power	BV and HV Connexion	voltage ratio	no-load loss	Loss of load	Short circuit voltage
160KVA	Δ/*Yn*	20/0.4KV	553W	2837W	5.58%

The equivalent representation model used in this study is shown in Figure 6. The measurements conducted by this author cover the frequency range of 100 kHz to 10 MHz and yield the following results.

- For the impedance represented by a parallel R, L, C circuit,

Table. 2 Measurement result

R_f	L_f	C_f
2210Ω	157mH	1.46nF

It should be noted that above 100 kHz, the transformer behaves as a simple R-L-C circuit; the magnetic circuits no longer function to transform currents and voltages according to the defined ratio for industrial frequencies.

- For different abilities,

Table. 3 Capacity measurement results.

C_1	C_2	C_{12-1}	C_{12-2}
36pF	*157mH*	*10pF*	*65pF*

To determine the transfer function of the quadrupole equivalent to our transformer, we use decibels (dB). Therefore, we normalize our results using the following expression [6]:

$$Transfer\ function = 20\log\left[\frac{V_{output}}{V_{input}}\right] \tag{7}$$

As source of excitation we use the voltage generator given by the following expression:

$$V_{Excitation} = \sum_{i=1}^{n} \sin(i.\omega.t) \tag{8}$$

n : It is the number of frequencies
$\omega = 2.\pi.f$
t : The time that encompasses all harmonics

Multi-wire line with (n+1) conductors

Consider an element of a uniform line represented by an elementary length (figure 9). We assume that the line is made up of $(n + 1)$ conductors whose $(n + 1)^{ième}$ conductor and reference conductor taken as ground plane [12].

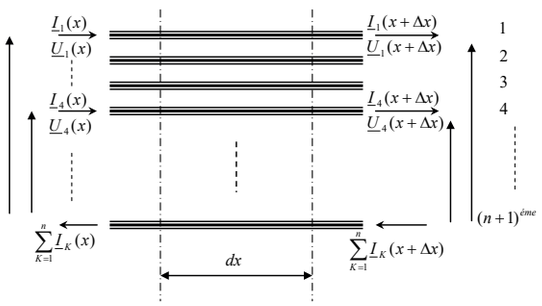

Fig. 9. Part of a multi-wire line

This element can be described by the equations (matrix form) of the following lines [12]:

$$\frac{d[\underline{U}(x)]}{dx} = -[\underline{Z}]\cdot[\underline{I}(x)] \tag{9}$$

$$\frac{d[\underline{I}(x)]}{dx} = -[\underline{Y}]\cdot[\underline{U}(x)] \tag{10}$$

With:
$[\underline{U}(x)]$: Complex vector of n order of phase stresses.
$[\underline{I}(x)]$: complex vector of order n of phase currents.
$[\underline{Z}]$ and $[\underline{Y}]$are the n-order matrices of admittances and linear complex impedances, they are symmetric.

Such as:

$$[\underline{Z}] = [R] + j.\omega.[L] \quad (11)$$

$$[\underline{Y}] = [G] + j.\omega.[C] \quad (12)$$

Or:

$[R]$ and $[L]$ are respectively the matrices of resistors and real n-order linear inductances.

$[G]$ and $[C]$ are respectively the matrices of conductance and real linear capacitances of order n.

Representation of a tube by the string matrix ϕ

Generally speaking, the chain matrix $\underline{\Phi}(L)$ expresses the currents and voltages at the output of the multipole as a function of their values at the input. For a line of length L, the voltages and phase currents at both ends of the line can be linked by the chain matrix $\underline{\Phi}(L)$, of order 2N, by the relation (13) [10]:

$$\begin{bmatrix}[\underline{U}(L)]\\ [\underline{I}(L)]\end{bmatrix} = \underline{\Phi}(L).\begin{bmatrix}[\underline{U}(0)]\\ [\underline{I}(0)]\end{bmatrix} = \begin{bmatrix}[\underline{\phi}_{11}(L)] & [\underline{\phi}_{12}(L)]\\ [\underline{\phi}_{21}(L)] & [\underline{\phi}_{22}(L)]\end{bmatrix}.\begin{bmatrix}[\underline{U}(0)]\\ [\underline{I}(0)]\end{bmatrix} \quad (13)$$

With:

$\underline{\varphi}^{ij}(L)$: Under matrix of order n.

The evaluation of [U(y)] et [I(y)], y =0 and y =L, and eliminating $\left[\underline{I}_m^{\pm}\right]$ we get the $\underline{\varphi}^{ij}(L)$.

The chain matrix is deduced after modal analysis. The essential task in solving MTL equations is to determine the expressions of sub-matrices given by [10]:

$$\left[\underline{\phi}_{11}(L)\right] = \frac{1}{2}[\underline{Y}]^{-1}.[\underline{T}].\left(e^{\underline{\gamma}_m L} + e^{-\underline{\gamma}_m L}\right).[\underline{T}]^{-1}.[\underline{Y}] \quad (14)$$

$$\left[\underline{\phi}_{12}(L)\right] = -\frac{1}{2}[\underline{Y}]^{-1}.[\underline{T}].\underline{\gamma}_m.\left(e^{\underline{\gamma}_m L} - e^{-\underline{\gamma}_m L}\right).[\underline{T}]^{-1} \quad (15)$$

$$\left[\underline{\phi}_{21}(L)\right] = -\frac{1}{2}[\underline{T}].\left(e^{\underline{\gamma}_m L} - e^{-\underline{\gamma}_m L}\right).\underline{\gamma}_m^{-1}.[\underline{T}]^{-1}[\underline{Y}] \quad (16)$$

$$\left[\underline{\phi}_{22}(L)\right] = \frac{1}{2}[\underline{T}].\left(e^{\underline{\gamma}_m L} + e^{-\underline{\gamma}_m L}\right).[\underline{T}]^{-1} \quad (17)$$

Representation of a tube by the string matrix (s)

In general, a two-port transmission line can be defined by [13]:

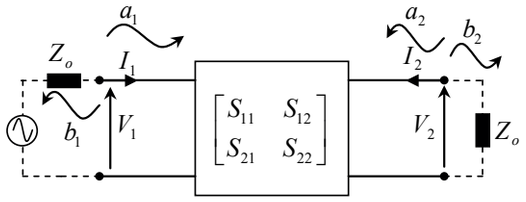

Fig. 10. Representation of a transmission line in voltage waves

$$\begin{cases} b_1 = S_{11}.a_1 + S_{12}.a_2 \\ b_2 = S_{21}.a_1 + S_{22}.a_2 \end{cases} \quad (18)$$

Or by a matrix representation:

$$\begin{pmatrix} b_1 \\ b_2 \end{pmatrix} = \begin{pmatrix} S_{11} & S_{12} \\ S_{21} & S_{22} \end{pmatrix}\begin{pmatrix} a_1 \\ a_2 \end{pmatrix} \quad (19)$$

Or :

b_1 : The voltage wave reflected at the quadrupole inlet;

a_1 : The voltage wave incident at the entry of the quadripôle;

b_2 : The voltage wave incident at the output of the quadrupole;

a_2 : The voltage wave reflected at the output of the quadrupole;

S_{11} : Reflection coefficient at the input when the output is adapted;

S_{22}:Reflection coefficient at the output when the input is matched;

S_{12} : Reverse transmission coefficient when the input is matched;

S_{21} : Direct transmission coefficient when output is matched;

The voltage waves mentioned above are calculated from the following expressions [12]:

$$\begin{cases} a_1 = \dfrac{V_1 + Z_0 I_1}{2\sqrt{\mathrm{Re}(Z_0)}} \\ a_2 = \dfrac{V_2 + Z_0 I_2}{2\sqrt{\mathrm{Re}(Z_0)}} \end{cases} \quad (20)$$

$$\begin{cases} b_1 = \dfrac{V_1 - Z_0^* I_1}{2\sqrt{\mathrm{Re}(Z_0)}} \\ b_2 = \dfrac{V_2 - Z_0^* I_2}{2\sqrt{\mathrm{Re}(Z_0)}} \end{cases} \quad (21)$$

With :

V_1 : Represents the voltage at the line input;

V_2 : represents the voltage at the output of the line,

From equations (19), the S parameters are obtained as follows:

$$S_{11} = \left.\frac{b_1}{a_1}\right|_{a_2=0} \quad (22)$$

Which represents the reflection coefficient at the input of the line knowing that the output of the line is adapted.

$$S_{22} = \left.\frac{b_2}{a_2}\right|_{a_1=0} \quad (23)$$

Which represents the reflection coefficient at the output of the line with a matched line input.

$$S_{12} = \left.\frac{b_1}{a_2}\right|_{a_1=0} \quad (24$$

Which represents the reverse propagation of the signal through the line, given that the input of the line is adapted.

$$S_{21} = \left.\frac{b_2}{a_1}\right|_{a_2=0} \quad (25) \quad \text{(III.31)}$$

Applications and results

Influence of the impact of the phase connection mode on the transfer function of the power transformer

The simulation using the EMTP-ATP software is performed with an electrical circuit-based approach and involves solving the nodal matrix equation [3]. For its applications, we tested several structures, labeled from H5 to H10. The difference between these structures lies in the injection point of the HF signal and the location where the response is measured. In our study, we present only two structures (H6 and H7). The modeling results obtained using EMTP-ATP software are validated through measurement.

Structure H6

In this simulation (figure 11), we inject the signal on the first phase of the LV side of the transformer and the signal recovery will be on the second phase of the MV side.

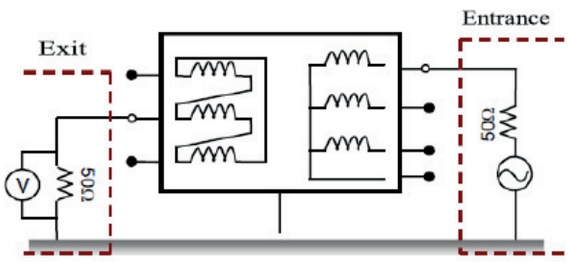

Fig. 11. H6 measurement diagram.

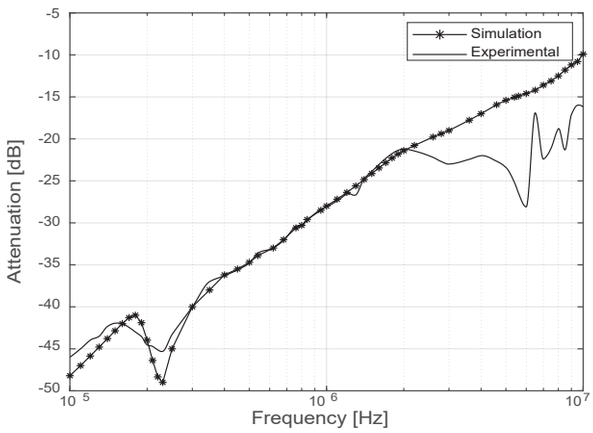

Fig. 12. Simulation and measurement of transformer transfer function variations (Structure H6)

Structure H7

The signal is now injected into the first phase on the MV side of the transformer, and the response is measured on the first phase of the LV side (figure 13).

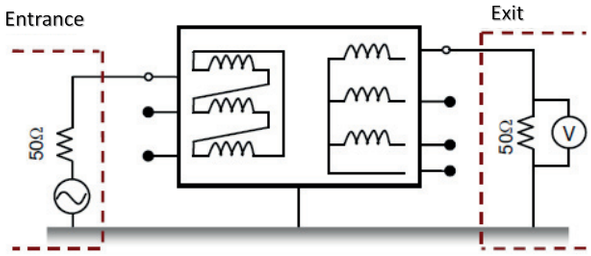

Fig. 13. H7 measurement diagram

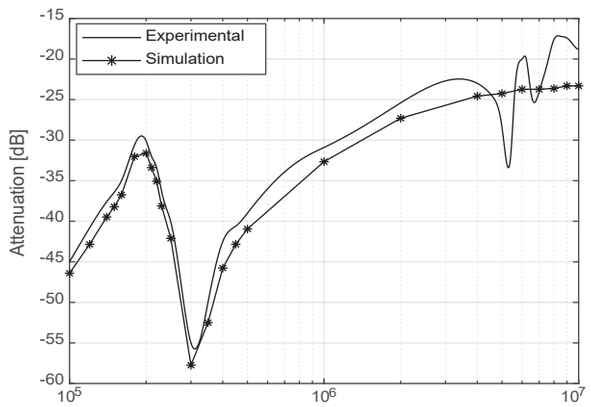

Fig. 14. Simulation and measurement of transformer transfer function variations (Structure H7)

Study of the propagation of the plc signal through a transformer equipped with its lines

In this part, we propose to study an electrical network consisting of a transformer equipped with its lines (input and output). This study will allow us to analyze:

The effect of the transformer;

- The effect of the number of departures;
- The effect of the network structure (looped or radial).

- Throughout the following study, we will use the H7 transformer structure, as it provides a better transformation ratio around 200 kHz, ensuring improved transformer performance.

Direct impact of the transformer on the transmission of the signal

To analyze the effect of the transformer on PLC signal transmission, we propose simulating the network shown in Figure 15 under two scenarios: first, without the transformer, and then with the power transformer present.. The line is of length L = 150m and of end load equal to the characteristic impedance of the line. The conductors have a conductivity equal to 5.10^7 *S/m* and that of the ground is $\sigma_s = 0.01$ *S/m*.

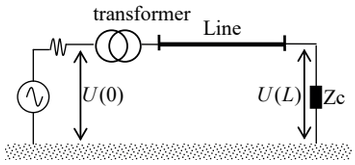

Fig. 15.The network studied during the simulation

Figure 16 below illustrates the variation of the transfer function with frequency, representing the ratio between the output voltage, denoted asU (L), and the input voltage, denoted as U (0).

For our simulation frequencies (>200 kHz), the transformation ratio is no longer relevant, as the magnetic circuit no longer plays a role at high frequencies. We can conclude that the transformer increases signal attenuation, as demonstrated by our results in figure 16.

Effect of the number of feeders

For this application, we propose to study the behavior of the network illustrated in figure 17 by varying the number of feeders (i.e. the number of loads). We analyze the variation of the ratio of the output voltage U (L) of the same feeder to the input voltage U (0), for several cases (1 feeder, 2 feeders, etc.).

The results in figure 18 clearly show that an increase in the number of branches (derivations) leads to greater attenuation in the propagation of the PLC signal. This can be explained by the variation of the output impedance with the number of connected connections; we note that the quality of the transmitted signal (CPL) degrades with the increase in departures, but with practically the same location of the resonances.

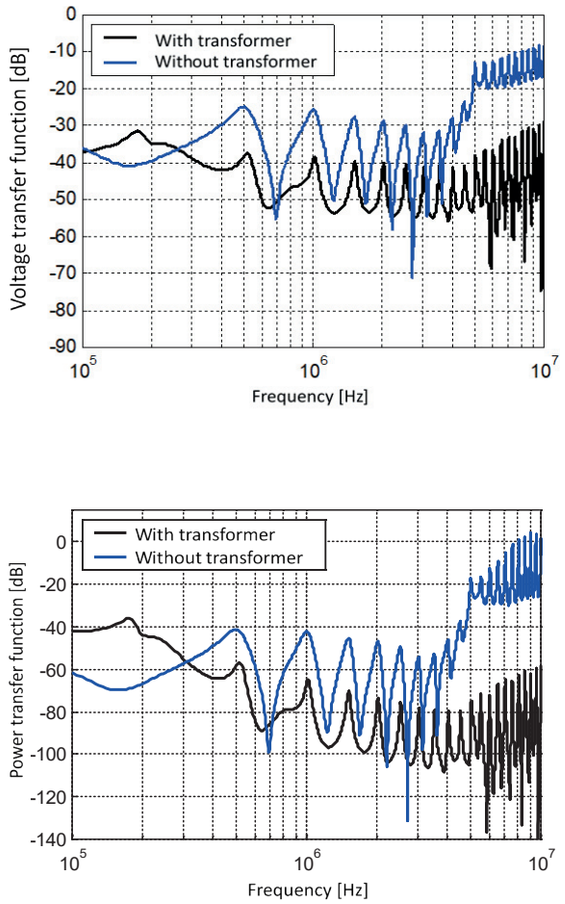

Fig. 16. Influence of the transformer on the propagation of PLC

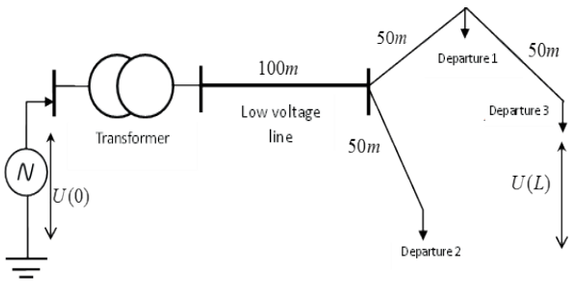

Fig. 17. Configuration studied during the simulation

Effect of network looping

In this final application, we analyze the effect of network looping on signal propagation. figure 19 illustrates the configuration of the proposed network. We examine the frequency variation of the transfer function (U (L)/U (0)) in two cases:

- Radial network
- Looped network

Analyzing the results in figure 20, we observe a clear improvement in the transfer function when the network is looped, indicating that signal transmission is more efficient in a looped network.

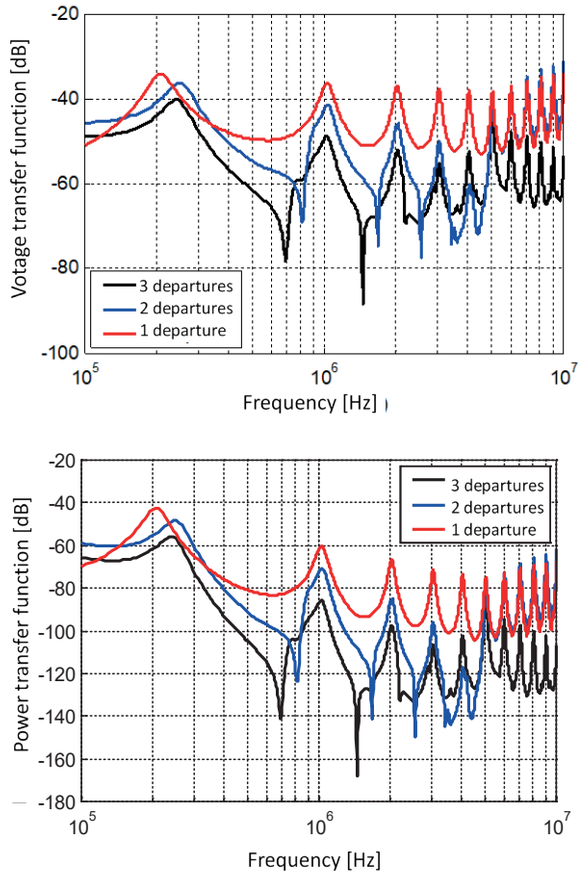

Fig. 18. Influence of the number of departures

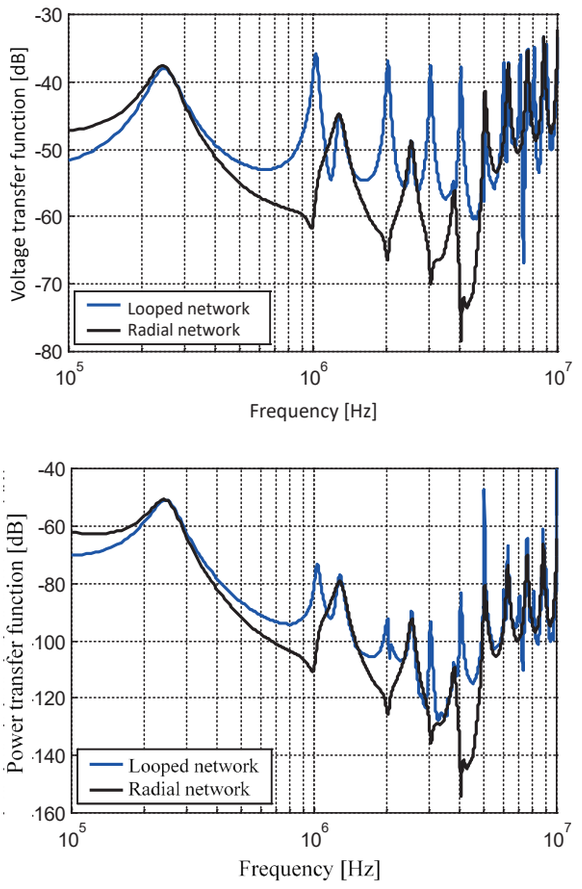

Fig. 20. Influence of network looping on the transfer function

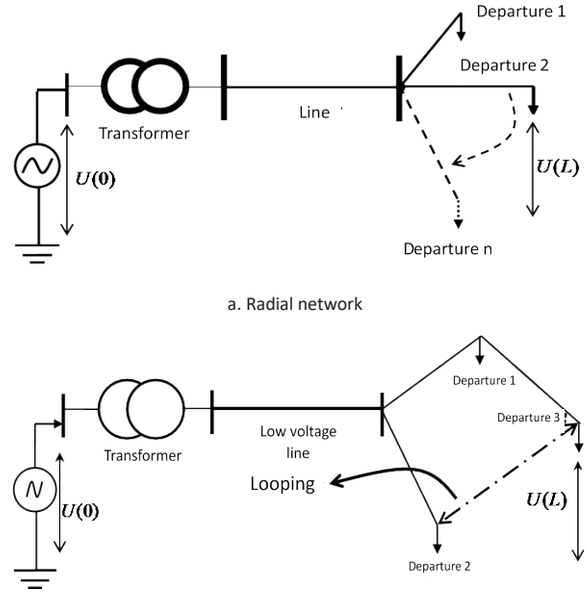

Fig. 19. Configuration of the networks studied during the simulation

Conclusion

Just as modeling electrical networks is challenging, modeling electrical equipment connected to the network is equally complex. This is because various types of equipment are randomly connected and disconnected, continuously altering the network load. Additionally, the characteristics of this equipment change over time, depending on factors such as its lifecycle, time of day, and frequency of use, sometimes making modeling unreliable. Therefore, it is crucial to develop a tool capable of modeling an entire electrical network, including its various cables and topology, to facilitate engineering analysis and enhance the understanding of PLC signal behavior on electrical cables.

We have therefore developed a MATLAB code that simulates the propagation of high-frequency (HF) signals on a network of lines or cables using the S-matrix method. To validate our theoretical developments, we have conducted several applications. For overhead lines, we tested signal propagation across different configurations. These applications have primarily allowed us to conclude that issues related to signal attenuation, bandwidth, and the effect of derivations can be effectively addressed by analyzing the transmitted power.

After analyzing our simulation and measurement results, we observed some discrepancies. A theoretical analysis of the approach used allowed us to iden-

tify the source of these differences. Consequently, we adopted an alternative approach that led to a significant improvement in the calculation results.

However, we encountered challenges in introducing the equivalent circuit, which significantly complicates the development of the structural data. Regarding the transformer and its associated lines, our calculations of the linear parameters ensure that the results are usable. Nevertheless, modeling using the S-matrix method would be more suitable, as it provides a more accurate characterization of high-frequency (HF) signal propagation.

Received: 22.03.2025, **Accepted:** 13.08.2025, **Published:** 29.08.2025

REFERENCES

[1] Chimklai S., Marti, J. R., Simplified three-phase transformer model for electromagnetic transients, IEEE Transaction on Power Delivery, 10 (1995), No. 3.
[2] Andrieu C., Boss D., A Frequency-Dependant Model For a MV/LV transformer", International Conference on Power Systems Transients (IPST), Budapest, Hungary (1999), 20–24.
[3] Tran-Anh T., Auriol P., Tran-Quoc T., Distribution network modelling for Power Line Communication applications". 9th International Symposium on Power Line Communications, Vancouver, Canada (2005), 4–6.
[4] Morched A., Marti L., Ottevangers J., A high frequency transformer model for EMTP". IEEE transaction on power delivery, 8 (1993), No. 3.
[5] Carson J. R., Wave Propagation in Overhead Wires With Ground Return", Bell system Techno Journal, 5 (1926), pp. 539–554.
[6] Potisk L., Hallon J., Orgon M., Fujdiak R., Electromagnetic compatibility of PLC adapters for in-home/domestic networks, Journal of Electrical Engineering, 69 (2018), No.1, pp.79–84.
[7] Sharma D., Dubey A., Mishra S., Mallik. R. K, A Frequency Control Strategy Using Power Line Communication in a Smart Microgrid, IEEE Access, 7 (2019), No.1, pp.21712– 21721.
[8] Henryk S., Lerch, A.Bień B., Monitoring of PV Inverters while Unintentional Islanding Using PMU", International Journal of Electronics and Telecommunications, 67 (2021), No.3, pp.465–470.
[9] Mahmood S. H., Salih A. M., KhalilM. I, Broadband services on power line communication systems", 22nd International Conference on Control Systems and Computer Science (CSCS), (2019), pp. 465–470.
[10] Cano C., Pittolo A., Malone D., Lampe L., Tonello, A.M., Dabak A.G., State of the Art in Power Line Communications: From the Applications to the Medium, IEEE Journal on Selected Areas in Communications, 34 (2016), No.7, pp.1935–1952.
[11] Wolkerstorfer M., Schweighofer B., Wegleiter H., Statovci D., Schwaiger H., Lackner W., Measurement and simulation framework for throughput evaluation of narrowband power line communication links in low-voltage grids, Journal of Network and Computer Applications, 59 (2016), No.2, pp.285–300.
[12] Sykora T., Husak M., Bastan O., Benes T., Automatic generation of a PLC controller based on a control system-identified model", Journal of Electrical Engineering, 72 (2021), No.2, pp.78–88.
[13] Paul C. R., Analysis of Multiconductor Transmission Lines, Wiley Interscience, 1994.
[14] Van der Merwe J., S-Parameters Measurements Yielding the Characteristic Matrices of Multiconductor Transmission Lines, IEEE trans. On Electromagnetic Compatibility, 40 (1998), No.3, pp. 249–255.
[15] Adesina L. M, Abdulkareem A., Ogunbiyi O., Effects of Ground Resistivity and Tower Structural Design on Transmission Line Symmetrical Components, International Journal of Recent Technology and Engineering (IJRTE), 9 (2020), No.1, pp.2115–2126.
[16] Xiao Z., Power communication network design considering global information fusion part two applications and explorations, Procedia Computer Science, 155 (2019), No.3, pp.768–773.
[17] Shekoni O. M., Hasan A.N., Shongwe T., Applications of artificial intelligence in power line communications in terms of noise detection and reduction, Aust. J. Electr. Electron. Eng., 15 (2018), No.1–2, pp. 29–37.